Oligo and polyuronic acids interactions with hypervalent chromium

Juan C. González [a], Silvia I. García [a], Sebastián Bellú [a], Ana María Atria [b], Juan Manuel Salas Pelegrín [c], Antal Rockenbauer [d], Lazlo Korecz [d], Sandra Signorella [a,*], Luis F. Sala [a,*]

[a] Instituto de Química de Rosario-CONICET, Universidad Nacional de Rosario, UNR, Suipacha 531, S2002LRK, Rosario, Argentina
[b] Facultad de Ciencias Químicas y Farmacéuticas-Universidad de Chile, Santiago de Chile, Chile
[c] Departamento de Química Inorgánica, Facultad de Ciencias, Universidad de Granada, Fuentenueva s/n, 18071 Granada, Spain
[d] Chemical Research Center, Hungary Academy of Sciences, Pusztaszeri street 59-67, H-1025 Budapest, Hungary

Keywords:
Chromium
Uronic acids
EPR
Redox chemistry
Kinetics

A B S T R A C T

Selective oxidation of galacturonic residues of oligo and polyuronic acids by Cr^{VI} affords CO_2/HCO_2H, oxidized uronic acid, and Cr^{III} as final redox products. Kinetic studies show that the redox reaction proceeds through a mechanism combining $Cr^{VI} \rightarrow Cr^{IV} \rightarrow Cr^{II}$ and $Cr^{VI} \rightarrow Cr^{IV} \rightarrow Cr^{III}$ pathways. The mechanism is supported by the observation of free radicals, CrO_2^{2+} and Cr^{V} as reaction intermediates. The EPR spectra show that five- and six coordinated oxo-Cr^{V} intermediates are formed. Penta-coordinated oxo-Cr^{V} species are present at any $[H^+]$, whereas hexa-coordinated ones are only observed at pH <1. At low pH Cr^{V} predominating species are coordinated by carboxylate groups and O^{ring} (g_{iso} = 1.9783/5). At pH 7.5, the predominating ones are those coordinated by alcoholate groups of the ligand (g_{iso} = 1.9800). Polygal can reduce Cr^{VI} and efficiently trap Cr^{III}. This behaviour represents an interesting model for the study of biomaterials, which possess a high proportion of polygal, in order to remove chromium from polluted waters.

1. Introduction

Uronic acids are widespread distributed in vegetal kingdom, composing the wall cell of higher plants, under polyuronic acid form [1]. Galacturonic acid (galur) is the major low-molecular-weight metabolite of pectic substances. The determination of the ability of galur residues to reduce or stabilise high oxidations states of Cr, will contribute to understand its potential role in the biochemistry of this metal. A high percentage of vegetal carbohydrates come from uronic acids and includes all the pectin material, gums, mucilage, hemicelluloses present in plants and microbiological polysaccharides [1]. Generally, the carboxylate groups present in galur residues, are under the form of calcium and magnesium complexes. Acid saccharides interaction with cations could be of great biological implications because metal complexation is probably taking place on the cell wall surface, rich in this kind of polysaccharides [2–4].

The Cr^{VI} coming from industrial waste produces a serious ambiental risk due to its toxicity and carcinogenicity [5]. Understanding the interaction of the galur residues with $Cr^{VI/III}$ could afford information over the biological and ecological implicancies of the presence of Cr on the environment. Remediation processes to remove hypervalent chromium in contaminated waters as, filtration, chemical precipitation, adsorption, electrochemical reduction and ionic exchange processes have been reported [6,7]. Adsorption is a versatile and efficient method to eliminate chromium, especially if the adsorbents which were used are economical [8]. The biomaterials employed in remediation, such as bagasse and materials coming from cellulose degradation, are winning importance as an economic alternative for the treatment of chromium contaminated water. Taking into account the carbohydrate capacity to bond Cr^{III} and reduce Cr^{VI} to Cr^{III}, the use of material rich in polysaccharide acid, in particular polymers of uronic acids, could be a new alternative for the chromium elimination from effluents [9].

2. Experimental

2.1. Materials

Sodium polygalacturonate (Sigma, 95%), digalacturonic acid (digal) (Sigma, 98%), trigalacturonic acid (trigal) (Sigma, 98%), potassium dichromate (Mallinckrodt), perchloric acid (A.C.S. Baker), 1,5-diphenylcarbazide (Aldrich, p.a.), acrylonitrile (Fluka 99%), 4-(2-hydroxyethyl-1-pyperazineetanesulfonic acid (Hepes) (Aldrich, 99.5%), diphenylpicrylhydrazyl (dpph) (Aldrich p.a.) glutathione, (GSH) (reduced form, Sigma 99.0%), oxygen peroxide

* Corresponding authors. Tel./fax: +54 341 4350214.
E-mail addresses: signorella@iquir-conicet.gov.ar (S. Signorella), sala@iquir-conicet.gov.ar (L.F. Sala).

(Merk, p.a.), chromium(III) nitrate nonahydrate (Aldrich 99%) and sulfuric acid (Cicarelli, p.a.), oxygen (99.99%). Aqueous solutions were prepared in milliQ deionised water (HPLC quality).

In experiments performed at pH 1–3, the pH of the solutions was achieved by addition of $HClO_4$ solution. In experiments at pH 7.0–7.5 the buffer used was 4-(2-hydroxyethyl-1-pyperazineetanesulfonic acid (Hepes). Concentration of stock solutions of $HClO_4$ was determined using standards analytical methods.

Caution: Cr^{VI} are human carcinogens, and Cr^{V} complexes are mutagenic and potential carcinogens [10]. Contact with skin and inhalation must be avoided. Acrylonitrile is a carcinogen and must be handled in a well-ventilated fume hood [11].

2.2. Methods

2.2.1. Spectrophotometric measurements

Spectrophotometric measurements were performed by monitoring absorbance changes using a Jasco-V-550 spectrophotometer with a fully thermostated cell compartment (±0.2 °C). Disappearance of Cr^{VI} in reactions with digal and trigal was followed spectrophotometrically at 350 nm under pseudo-first-order conditions, using at least a 50-fold molar excess of substrate over Cr^{VI}. Reactant solutions were previously thermo stated and transferred into a 1.0 cm path length cell immediately after mixing. Experiments were performed at 33 °C unless otherwise stated and mixtures of sodium perchlorate and perchloric acid were used to maintain a constant ionic strength (I) 1.0 M. The disappearance of Cr^{VI} was followed until at least 80% conversion. In the kinetic measurements, the initial concentration of Cr^{VI} was kept at 6.0×10^{-4} M and the digal/trigal concentration was varied from 0.03 to 0.09 M, [$HClO_4$] was kept constant at 0.2 M. Multiple measurements showed the reproducibility of the method. Rate constant (k_6, k_5) were deduced from multiple determinations and were within ±10% error for each other. The first-order dependence of the rate upon [Cr^{VI}] was verified in a set of experiments where the $[Cr^{VI}]_0$ was varied between 0.3 and 0.6 mM but temperature, $[digal]_0$ or $[trigal]_0$, [H^+] and I were kept constant.

The presence of superoxoCr^{III}, CrO_2^{2+}, in mixtures of digal or trigal/Cr^{VI} was investigated by periodic scanning UV–Vis spectrophotometry in the 220–500 nm region of O_2-saturated solutions, 1.26 mM, containing 0.1 M digal or trigal, [$HClO_4$] = 0.2 M, [Cr^{VI}] = 0.047 mM, I = 1.0 M at 25 °C. Periodic scanning of the reaction mixture showed that the Cr^{VI} band at 350 nm decreased in intensity, while new peaks at 290 and 247 nm, characteristic of CrO_2^{2+} grew in.

2.2.2. Chromium determination in polygal/Cr^{VI} supernatant mixtures

Perchloric acid used in the reaction mixture of polygal/Cr^{VI} protonates the carboxylate groups of polygal, producing its aggregation in particles of different sizes, which depends on the experimental conditions. In all experiences, polygal was generated by direct reaction of sodium polygalacturonate solutions with perchloric acid. Different mass of sodium polygalacturonate (25–1200 mg) were dissolved in 31.0 mL of distilled water at 60 °C, with constant stirring. 1.10 mL of $HClO_4$ 3.83 M was added to a heterogeneous mixture, which was then incubated for 10 min. Finally, 2.0 mL Cr^{VI} 0.30 M was added. The final composition of the mixture was [$HClO_4$] = 0.12 M, [Cr^{VI}] = 0.0176 M, [polygal] = 0.73–35.2 g/L. Reaction mixture was kept in close recipients thermostitazed at 60 °C. After 24 h of stirring, 2.0 mL aliquot of the suspension were centrifuged during 30 min at 5000 rpm. About 200–300 μL of the clear supernatant were taken and dried in a porcelain cap and calcinated until total elimination of organic material. The yellow solid [12] was taken up to a final volume of 5.0 mL with H_2SO_4 0.10 N and measurements of the absorbance at 350 nm allowed calculation of the [Cr^{VI}].

2.2.3. EPR measurements

The EPR spectra were obtained on a Bruker EMX0 spectrometer operating at X-band frequencies (∼9–10 GHz). Microwave generation was means with a Bruker 04 ER and measured with a Bruker EMX 048T frequency meter. Spectra were recorded as first derivatives of the microwave absorption in 1024 point at 20 ± 1 °C using 10 mW microwave power, 100 kHz modulation frequency, and 0.29–2.00 G modulation amplitude. *g*-Values were determined by reference to (dpph) (g_{iso} = 2.0036) as an external standard. In EPR measurements, scanning speed and scans number were fixed in order to reduce the time used in each measurement. This was done to avoid fluctuations in the EPR signal during the sample scanning. Power values used in the EPR experiments did not overcome 10 mW in order to avoid signal saturation.

Long-lived oxo-Cr^{V}-oligouronic and polygal complexes were generated by reaction of $K_2Cr_2O_7$ with an aqueous solution containing GSH at 25 °C. In the experiments [Cr^{VI}] = [GSH]. Final concentration in mixtures polygal/GSH/Cr^{VI}, where [Cr^{VI}] = [GSH] = 0.012–0.014 M; [polygal] = 19.2–23.0 g/L.

All the EPR spectra were simulated using the PEST WINSIM [13] program assuming 100% Lorentzian line shapes. The spectral parameters for each Cr^{V} species were similar in all simulations, with a maximum deviation of ±0.0001 in the g_{iso} values. Values for a_{iso} (^{1}H) were included in the simulations only when were greater than the line width of the oxo-Cr^{V} species.

2.2.4. Polymerization test

The presence of free radicals in the reactions of digal and trigal with Cr^{VI} was tested by acrylonitrile polymerization test. About 0.2 mL of acrylonitrile was added to a solution of Cr^{VI} (0.0027 mmol) and digal/trigal (0.07 mmol) in $HClO_4$ 0.20 M (0.5 mL). After a few minutes at 33 °C, a white precipitate appeared. 0.5 mL of acrylonitrile was added to a reaction mixture containing 53.1 g/L of polygal and 8.0 mM of Cr^{VI}, in 2.0 mL of $HClO_4$ 0.01 M. The mixture was left 2.0 h at 60 °C. After this time, the white precipitate could be seen. ^{13}C NMR of a D_6-DMSO solution of the white solid and FT-IR of the solid showed the pattern characteristic of polyacrilonitrile. Blank experiments with either Cr^{VI} or polygal gave no detectable white precipitates. Control experiments (without Cr^{VI} or reductant present) did not show the formation of a precipitate. The possible reaction of Cr^{V} or Cr^{IV} with acrylonitrile was tested with Na[$Cr^{V}O(ehba)_2$] [14] and [$Cr^{IV}O(ehba)_2$] [15] (ehba = 2-ethyl-2-hydroxybutanoic acid). No precipitation occurred on mixing the Cr^{V} or Cr^{IV} complexes with acrylonitrile under the same conditions as those used in the Cr^{VI} + digal/trigal/polygal reactions.

2.2.5. Effect of external reducing agent (Na_2SO_3) in polygal/Cr^{VI} mixture

Reaction mixture of polygal and perchloric acid were 35.2 mg/L and 0.12 M, respectively. About 0.9 mmol of Na_2SO_3 and 2.0 mL of Cr^{VI} solution 0.3 M were added to 34.1 mL of the reaction mixture.

2.2.6. HCO_2H and CO_2 determination in polygal/Cr^{VI} mixtures

Supernatant of polygal/Cr^{VI} reaction mixture was employed to analyse oxidation products. Carbon dioxide was measured in 35.0 g/L polygal and Cr^{VI} 2.90 mmol/L mixture, in $HClO_4$ 0.12 M. The reaction mixture was continuously stirred and flushed with pure nitrogen at 60 °C. Gaseous products were passed trough three flasks containing NaOH solution. Once the reaction finished, NaOH solutions were titrated with standard HCl in order to determine the carbon dioxide generated. Supernatant was filtered employing a 0.2 μm of porous diameter membrane and analysed by HPLC, showing the presence of formic acid with retention time (R_t) 13.20 min. An aminex HPX-87H column at 25 °C and 0.6 mL/min flow, detection at 220 nm, was used for this experiment. Co

chromatography of polygal reaction mixture with a formic acid solution of known concentration afforded an increment in the 13.20 min peak, confirming identity of detected product. Additionally supernatant polygal/Cr^{VI} reaction mixture was taken to pH 2 with KOH 0.5 M, filtrated to eliminate $KClO_4$ and then distilled. To 5.0 mL of the distillate, 1.0 mL of $HgCl_2$ (2.0%) was added at 80 °C and a white precipitate of Hg_2Cl_2 was observed, which indicate the presence of a reducing compound [16]. Peak area versus [HCO_2H] calibration curves were obtained by HPLC and used for formic acid quantification.

3. Results and discussion

3.1. Digal, trigal or polygal/Cr^{VI} reaction intermediates

Time-dependent UV/Vis spectra of digal/Cr^{VI} and trigal/Cr^{VI} reaction mixtures showed absorbance decrease at 350 nm and 420–470 nm, while absorbance at 570 nm increased, without an isosbestic point, Fig. 1.

The lack of an isosbestic point indicated that there were two or more competing reactions at any time and that, intermediate chromium species coming from Cr^{VI} to Cr^{III} reduction, were present in appreciable concentrations. At the end of reaction, two d–d-bands ascribed to Cr^{III} were observed at λ_{max} 411 nm (ε = 17.5 M^{-1} cm^{-1}) and λ_{max} 570 nm (ε = 15.2 M^{-1} cm^{-1}), corresponding to $^4A_{2g} \rightarrow {}^4T_{1g}$ and $^4A_{2g} \rightarrow {}^4T_{2g}$ transitions of $[Cr(OH_2)_6]^{3+}$ ion [17]. Therefore, it was confirmed that Cr^{III} aqua ion was the only inorganic product under our experimental conditions.

3.1.1. Oxo-Cr^V species characterization by EPR spectroscopy

Presence of oxo-Cr^V-di or trigal species can be identified with great sensitivity by EPR spectroscopy, where strong and narrow isotropic signals were observed at room temperature in X-band spectra. Assignment of the structures of the oxo-Cr^V species in solutions have, therefore, been made on the basis of the isotropic EPR parameters g_{iso}, A_{iso} and $^1Ha_{iso}$.

3.1.1.1. Digal chromium(V) complexes. Multiplicity of EPR signals of digal/Cr^{VI} reaction mixture at pH 1–3 could not be resolved because the shf coupling constants were lower than the line width. Spectra were simulated with three singlets in order to obtain information from the average g_{iso} values of oxo-Cr^V species in the reaction mixture. At pH 7.0, EPR signals showed lower line width, and $^1Ha_{iso}$ values were obtained. Table 1 shows the results obtained from the experimental spectra simulation (Fig. 2).

The ^{53}Cr A_{iso} value belonging to oxo-Cr^V/digal species was 17.3×10^{-4} cm^{-1}, characteristic of oxo-Cr^V pentacoordinate species [18–21]. This result was in agreement with previous works where it was found that five-coordinated oxo-Cr^V species have higher g_{iso} and lower ^{53}Cr A_{iso} values than the corresponding six-coordinated species [21–23]. Taking into account spectral parameters, we were able to assign the g_{iso} 1.9780/1.9784 to a bischelate, where digal bounds an oxo-Cr^V through the carboxylate group and the oxygen of pyranosic ring Fig. 3a. Considering that digal acid is under the pyranosic form in water [24], coordination through the fragment of β-hydroxiacids was discarded because it implies formation of a six member chelate ring, which it is not a favourable situation [21]. g_{iso} = 1.9788 value belongs to a bischelate pentacoordinate oxo-Cr^V species, bound to carboxylate group and three alcoxy group [21], [$Cr^VO(O^{6(6')}$, O^{ring}-digal)/$O^{1'(3)}$,$O^{2'(4)}$-digal) (Fig. 3b).

At pH 7.0 the digal/Cr^{VI} reaction mixture afforded oxo-Cr^V complexes coordinated to a diolate group where the triplets were assigned to species [Cr^VO(*cis*-$O^{1'(3)}$,$O^{2'(4)}$-digalacturonate)$_2$] and mixed species [Cr^VO(*cis*-$O^{1'}$,$O^{2'}$-digalacturonate)(*cis*-O^3,O^4-digalacturonate)]$^-$ (Fig. 4).

3.1.1.2. Trigal chromium(V) complexes. Table 2 shows the results obtained after simulation of the EPR signals at different pH value (Fig. 5).

At pH 2.0 the mayor species (73.8%) presents a g_{iso} 1.9786 value. This signal was assigned to a bischelate of oxo-Cr^V pentacoordinate, where the metal is being bound by two molecules of trigal, through carboxylate groups and a ring oxygen [$Cr^VO(O^{CO2}$, O^{ring}-trigal)$_2$]$^-$. The other species with g_{iso} 1.9790/3 in a minor proportion was ascribed to [Cr^V $O(O^{CO2}$, O^{ring}-trigal)(*cis*-O–O-trigal)]$^-$ complex. At pH 3.0, the EPR spectrum shows that the species [Cr^V $O(O^{CO2}$, O^{ring}-trigal)$_2$]$^-$(g_{iso} 1.9786) and [$Cr^VO(O^{CO2}$, O^{ring}-trigal)(*cis*-O,O-trigal]$^-$(g_{iso}1.9792) were preponderant. A triplet signal at g_{iso} 1.9796 was assigned to [Cr^VO(*cis*-O,O-trigal)$_2$]$^-$ species. At pH 4.0, the proportion of species [Cr^VO(*cis*-O,O-trigal)$_2$]$^-$ (g_{iso} 1.9796 and 1.9800) were 39% of the $[Cr^V]_T$ in the reaction mixture, meanwhile at pH 7.0 the species of oxo-Cr^V-*cis*-diolate afforded the 100% of the $[Cr^V]_T$ in the solution. So, oxo-Cr^V species distribution with pH follows the same tendency observed in others uronic acids and polyhidroxocarboylic compounds [25].

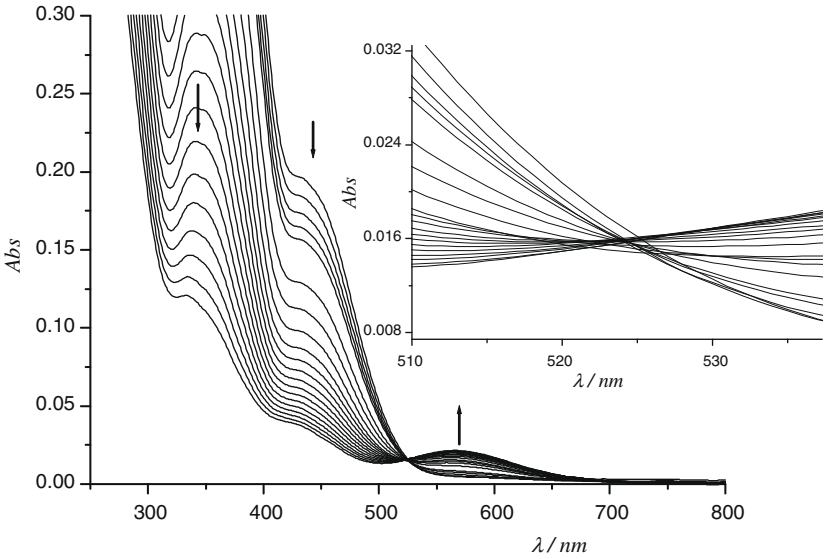

Fig. 1. Time evolution of the UV/Vis spectra from a mixture of trigal (0.04 M) and Cr^{VI} (1.35 mM) over a period of 2.0 h; [$HClO_4$] = 0.20 M; T = 33 °C and I = 1.0 M.

Table 1
EPR spectral parameters for Cr^{V} intermediates in the digal/Cr^{VI} reactions. [Cr^{VI}] = [GSH] = 0.97 mM; [digal] = 0.19 M; [digal] = 0.28 M; I = 1.0 M; T = 20 °C; mod. amp. = 0.40 G; $\nu \approx$ 9.76–9.38 GHz; s = singlet; t = triplet.

pH	g_{iso}	Multiplicity	$^{1}Ha_{iso}$ (10^{4} cm^{-1})	%
1	1.9788/1.9784/1.9780	s		64.3/26.7/9.0
2	1.9788/1.9784/1.9780	s		72.2/20.9/6.9
3	1.9788/1.9784/1.9780	s		71.0/20.3/87
7*	1.9800/1.9798/1.9796	t/t/t	0.84/0.51/0.82	17.0/22.8/60.2

* [Cr^{VI}] = [GSH] = 5.59 mM.

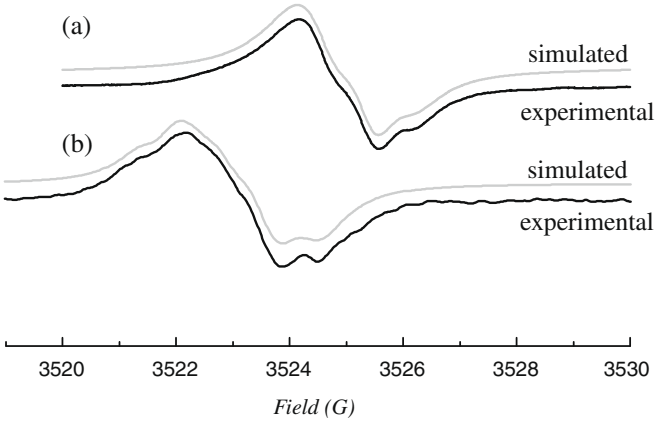

Fig. 2. Experimental and simulated X-band EPR spectra of mixtures digal/Cr^{VI}: (a) pH 3; [Cr^{VI}] = [GHS] = 1.22 mM; [digal] = 0.19 M; (b) pH 7; [Cr^{VI}] = [GSH] = 5.59 mM; [digal] = 0.28 M. T = 20 °C; $\nu \approx$ 9.76 GHz; I = 1.0 M; mod. amp. = 0.40–0.29 G.

3.1.1.3. Polygal chromium(V) complexes. EPR spectra of polygal with Cr^{VI} reaction mixture showed more complex and less resolved signals than in the former system. In general, the signals were very wide at every concentration of protons studied, which indicated the contribution of several Cr^{V} isomers. In a polygal/Cr^{VI} reaction mixture at pH 2–3, after 20 h of reaction, EPR spectra were composed by three signals (Fig. 6), g_{iso} values presented in Table 3.

The signal with average g_{iso} = 1.9783/5 belongs to species where the oxo-Cr^{V} was coordinated to two alcoxo groups and two carboxylate groups, meanwhile the signal with average g_{iso} = 1.9752/7 belongs to [$Cr^{V}O(O^{CO2}$,O-polygal)$(H_2O)_2]^{+}$ specie. Unlike the results observed in the olygomers, there was approximately a 20% of species in this pH range, where the oxo-Cr^{V} group is being coordinated with four alcoholate groups (g_{iso} 1.982–1.981) at the beginning of the reaction. As it is observed on Fig. 7, the proportion of species with average g_{iso} = 1.9783/5 increases with time, meanwhile the others decreases, at 50 h the species oxo-Cr^{V}-$(O_2CR)_2$ are clearly predominant.

The numerous chelating sites and the flexibility of the polymer chain, allowed the formation of several oxo-Cr^{V} species, coordinated with α-hydroxycarboxylate and diolates at acidic pH. Anyway, the predominant species with g_{iso} 1.9783 during reaction time, indicated that the coordination mode of $Cr^{V}O(O^{CO2}$, O^{ring}-polygal$)_2]^{-}$ was the most suitable from the thermodynamic point of view at acidic pH. Reaction mixture of polygal/Cr^{VI}/GSH at pH 7.0, showed an average g_{iso} = 1.9796. Fig. 8 shows time evolution of a reaction mixture of GSH/Cr^{VI} in presence of polygal.

In this figure, it is possible to notice that Cr^{V} produced by redox reaction between Cr^{VI} and GSH was coordinated faster by GSH than by the polymer. The specie Cr^{V}–GSH (g_{iso} 1.9857) exchanged GSH for polygal, affording g_{iso} = 1.9796, which belongs to species of oxo-Cr^{V} coordinated to four alcoholate groups. Therefore, at pH 7.0, average g_{iso} value indicates that coordination between Cr^{V} and polygal took place mainly through the alcoholate groups of the ligand.

3.2. Intermediacy of Cr^{II}

It is known that Cr^{IV} oxidizes alcohols as a two-electron oxidant to yield Cr^{II} and the oxidized organic product. The fact that Cr^{II} is

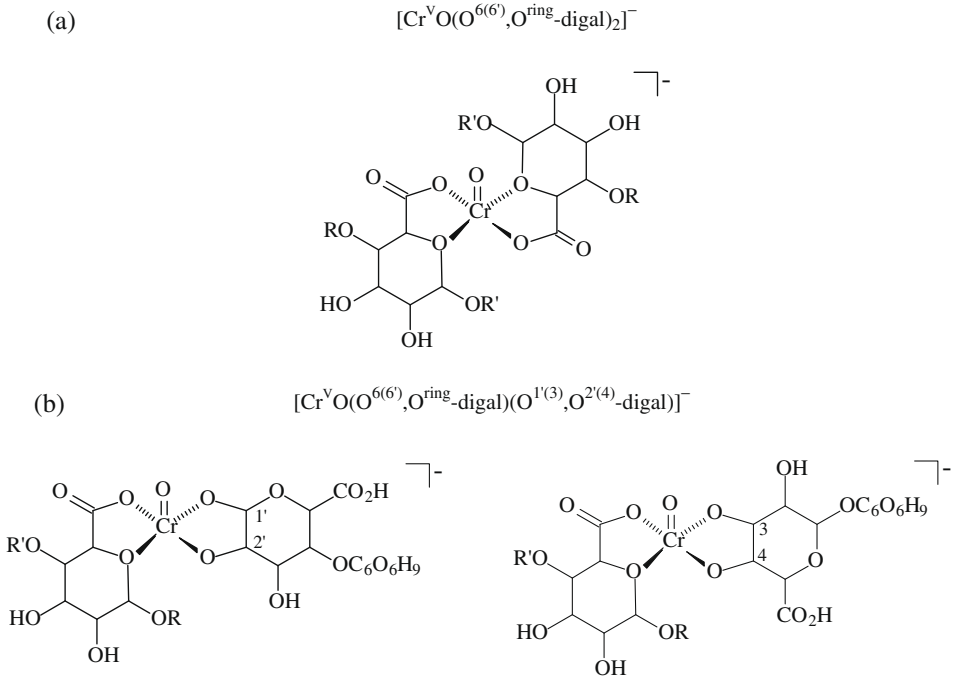

Fig. 3. Structures of Cr^{V} complexes with digal at pH 1–3. R = H and R′ = $C_6O_6H_9$ (coordination through the reducing residue) or R = $C_6O_6H_9$ y R′ = H (coordination through the non reducing residue).

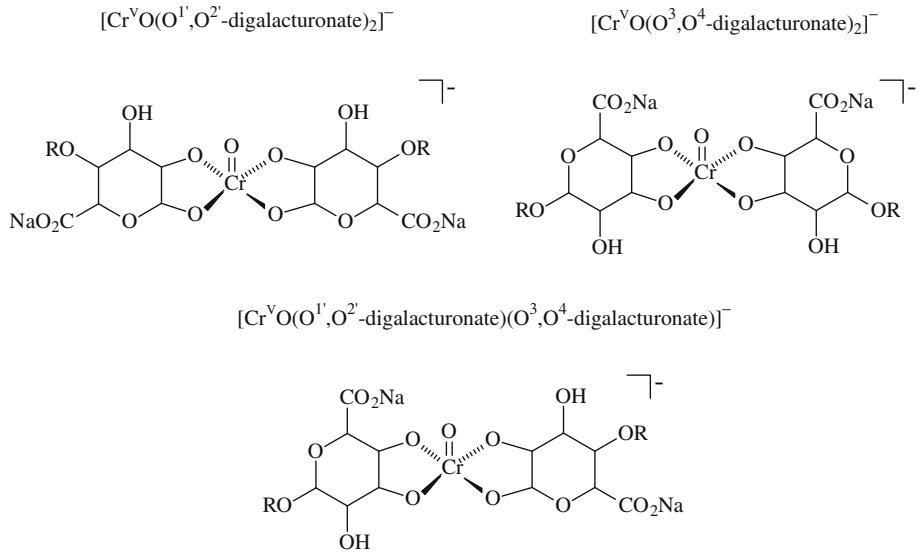

Fig. 4. Structures of Cr^{V} complexes with digal at pH 7.

involved in the oxidation mechanism of several alcohols by Cr^{IV} and Cr^{VI} in $HClO_4$ was demonstrated by conversion to CrO_2^{2+} upon reaction with molecular oxygen [26–30]. At high $[O_2]$ and low $[Cr^{VI}]$ the reaction of Cr^{II} with O_2 can compete successfully with the reaction of Cr^{II} with Cr^{VI} and the autocatalytic consumption of CrO_2^{2+} by Cr^{II}. If Cr^{II} is intermediate specie in the redox reaction, CrO_2^{2+} should be detected. The interdemiacy of Cr^{II} in the reaction of digal or trigal with Cr^{VI}, was monitored by the formation of CrO_2^{2+}, using low $[Cr^{VI}]$ and high $[O_2]$. A periodic scanning of O_2-saturated solution (1.26 mM) of a Cr^{VI} + digal or trigal reaction mixture in 0.20 M $HClO_4$ showed two absorption bands at 290 and 247 nm, characteristic of CrO_2^{2+} (Fig. 9).

Inset Fig. 9 shows CrO_2^{2+} absorption at 247 nm versus time. CrO_2^{2+} absorbance at 247 nm was calculated in the following way:

Table 2
EPR spectral parameters for Cr^{V} intermediates in the trigal/Cr^{VI} reactions. $[Cr^{VI}]$ = [GSH] = 1.22 mM; [trigal] = 0.19 M; I = 1.0 M; T = 20 °C; mod. amp. = 0.29 G; $\nu \approx 9.76$ GHz; t = triplet; s = singlet.

pH	g_{iso}	Multiplicity	$^{1}Ha_{iso}$ (10^4 cm^{-1})	%
2	1.9786	s		73.8
	1.9790	s		25.0
	1.9793	s		1.20
3	1.9786	s		68.2
	1.9792	s		29.0
	1.9796	t	0.78	2.70
4	1.9786	s		61.1
	1.9796	t	0.73	31.6
	1.9800	t	0.67	7.40
7	1.9800	t	1.02	25.7
	1.9796	t	0.94	74.3

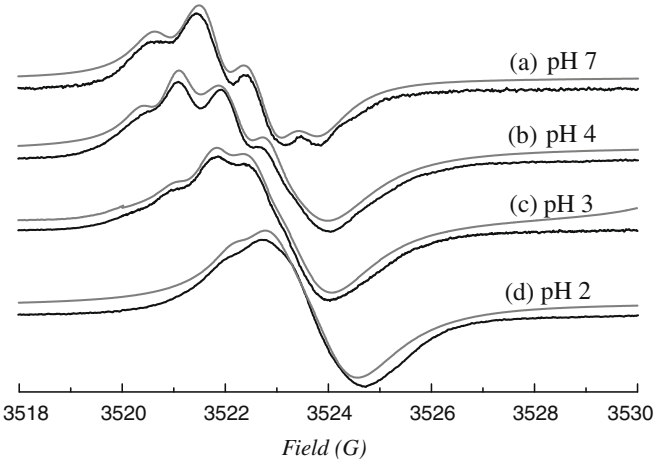

Fig. 5. Experimental and simulated X-band EPR spectra of mixtures trigal/Cr^{VI}; .$[Cr^{VI}]$ = [GHS] = 1.22 mM; [trigal] = 0.19 M; I = 1.0 M; T = 20 °C; mod. amp. = 0.29 G; $\nu \approx 9.76$ GHz; $^{*}[Cr^{VI}]$ = [GSH] = 1.22 mM.

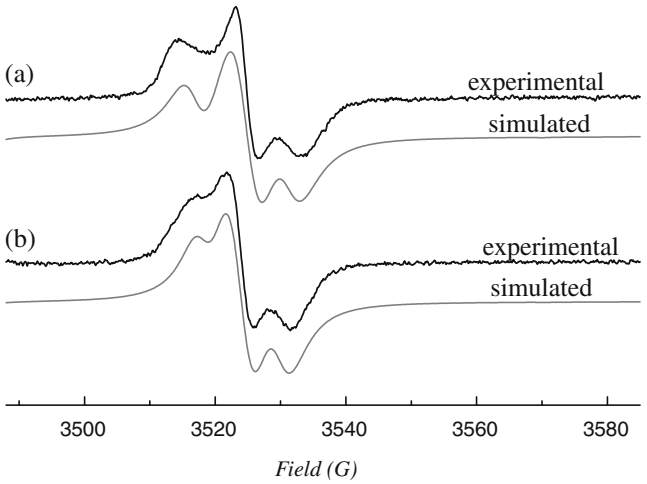

Fig. 6. Experimental and simulated X-band EPR spectra of mixtures polygal/Cr^{VI}; [polygal] = 19.2 g/L; [GHS] = $[Cr^{VI}]$ = 0.012 M; $\nu \approx 9.76$ GHz; T = 20 °C; mod. amp = 2.0 G; t = 20 h. (a) pH 2; (b) pH 3.

Table 3
EPR spectral parameters for Cr^{V} intermediates in the polygal/Cr^{VI} reactions [polygal] = 30.0 g/L; $[Cr^{VI}]$ = 0.975 mM; t = 20.0 h; $\nu \approx 9.76$ GHz; T = 20 °C; mod. amp. = 2.0 G.

	g_{iso}	%		g_{iso}	%
pH 2	1.9783	47.5	pH 3	1.9785	39.1
	1.9752	32.0		1.9757	38.0
	1.9820	20.5		1.9811	22.9

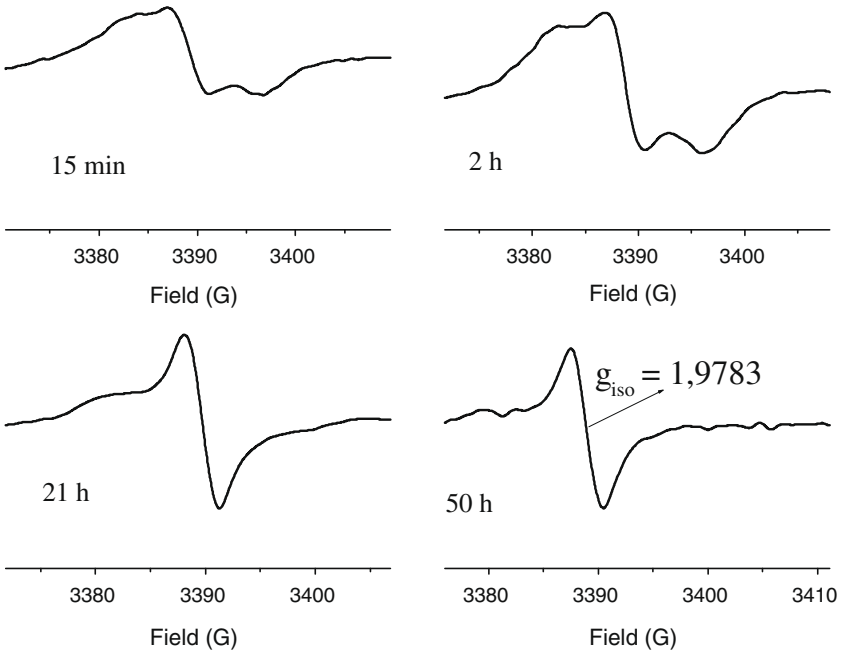

Fig. 7. EPR espectra time evolution of oxo-Cr^{V}-polygal species at acidic pH.

$$Abs^{247}(CrO_2^{2+}) = Abs^{247} - Abs^{350} \times (\varepsilon 1)^{-1} \times (\varepsilon 2)$$

where $\varepsilon 1$ and $\varepsilon 2$ represent the molar absorption coefficient of Cr^{VI} at 350 and 247 nm, respectively. In the experimental condition used $\varepsilon 1 = 1550\ M^{-1}\ cm^{-1}$ and $\varepsilon 2 = 1900\ M^{-1}\ cm^{-1}$. Keeping in mind that the molar absorption coefficient of CrO_2^{2+} at 247 nm is 7000 $M^{-1}\ cm^{-1}$ [27], the maximum concentration of CrO_2^{2+} (t_{max} = 12.1 - min) was 37%.

These spectroscopic results showed that Cr^{II} was produced in the redox reaction and this fact was taken as evidence that Cr^{IV} was implied in the redox mechanism of digal or trigal oxidation by Cr^{VI} in acidic media. The yielding of CrO_2^{2+} is expected to approach 100% if the reaction takes place exclusively through the $Cr^{VI} \rightarrow Cr^{IV} \rightarrow Cr^{II}$ pathway [27]. In these reactions $[CrO_2^{2+}]_{max}$ reached a value of 37% suggesting that one half of the $HCrO_4^-$ was reacting through a pathway that involved Cr^{II} .This behaviour was observed in another related systems [31]. Under the present kinetic measurements conditions, Cr^{IV} reacted with digal or trigal much faster than Cr^{VI}. High reactivity of Cr^{IV} against alcohols and aldehydes [27], neutral carbohydrates, aldonic, uronic, aldaric acids [32] and polysaccharides [33] has been experimentally demonstrated. This implies that Cr^{V} was the only chromium intermediate that accumulates in the reaction mixtures as can be seen by EPR.

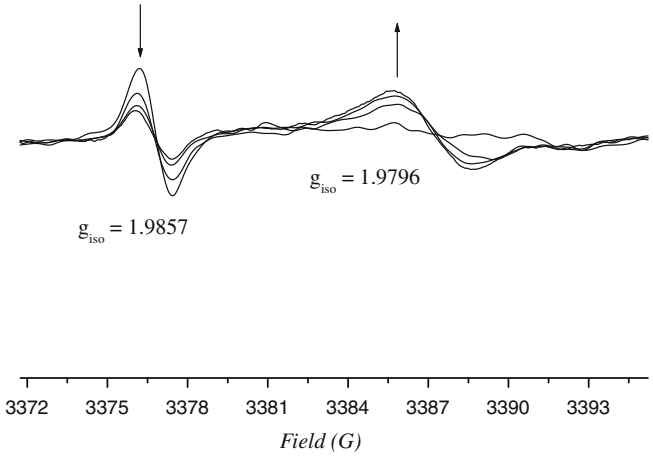

Fig. 8. EPR espectra time evolution of polygal/Cr^{VI}/GSH mixtures at pH 7.

3.3. Rate studies

Absorbance curves versus time at 350 nm of the digal or trigal/Cr^{VI} mixtures showed a monotonic decrease which cannot be described by a single exponential decay. These kinetics profiles were adequately described by the set of consecutive first-order reactions of Scheme 1. It is known that Cr^{V} species absorb strongly at 350 nm and may superimpose Cr^{VI} absorbance yielding the wrong interpretation of spectrophotometric absorbance decay values, especially when the Cr^{VI} and Cr^{V} decay rates are of the same order [34]. So, considering the Cr^{V} absorption superimposition, the absorbance at 350 nm, at any time during the redox reaction, is given by:

$$Abs^{350} = \varepsilon^{VI}[Cr^{VI}] + \varepsilon^{V}[Cr^{V}] \quad (1)$$

Combining Eq. (1) with rate expressions [35] derived from Scheme 1 yields

$$Abs^{350} = Abs_0 e^{-2k6t} + k_6 \varepsilon^{V}[Cr^{VI}]_0 (e^{-k5t} - e^{-2k6t})/(2k_6 - k_5) \quad (2)$$

In Eq. (2), ε^{V} refers to the molar absorptivity of Cr^{V}-digal or Cr^{V}-trigal at 350 nm (ε^{V} 1800 $M^{-1}\ cm^{-1}$). Parameters k_6 and k_5 refer to the rate of disappearance of Cr^{VI} and Cr^{V}, respectively, and were evaluated from a non-linear iterative computer fit of Eq. (2). It must be noted that in Eq. (2), k_6 appears in the numerator of the pre-exponential term and $2k_6$ appears in the denominator and in the exponential terms because, according to the proposed reaction scheme, only half of the Cr^{VI} reaches Cr^{III} through a Cr^{V} intermediate. At $HClO_4$ 0.2 M, in the 0.03–0.09 M digal or trigal range, the calculated values of k_6 and k_5 were very close ($k_6/k_5 \approx 2.50$–$1.95/1$). This fact implied that the slow redox steps involved the reduction of Cr^{VI} and Cr^{V}. The simulation of the kinetic profiles employing k_6 and k_5 values obtained from Eq. (2), showed that the maximal $[Cr^{V}]$ represented 33.3% of the total Cr in $HClO_4$ 0.2 M and trigal 0.09 M (Fig. 10).

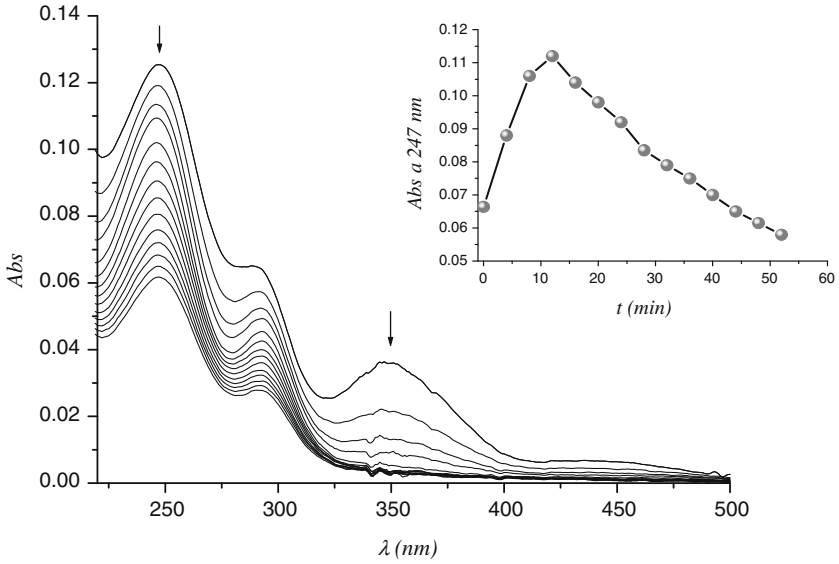

Fig. 9. CrO_2^{2+} formation of (λ_{max} 290, 247 nm) from the reaction between 0.10 M trigal, 1.26 mM O_2, 0,20 M $HClO_4$ and 0.047 mM Cr^{VI}, at 25 °C and I = 1,0 M. Spectra recorded every 4 min. Inset shows CrO_2^{2+} absorption at 247 nm vs. time.

$$2\,Cr^{VI} \longrightarrow Cr^{V} + Cr^{III} \longrightarrow Cr^{III}$$

Scheme 1.

These results were consistent with the fact that absorbance at 350 nm reflects changes in [Cr^{VI}] and [Cr^{V}]. The calculated kinetics parameters, k_6 and k_5, for various [trigal] and [digal] at fixed [$HClO_4$] are summarized in Table 4.

In 0.1 M $HClO_4$, the Cr^{V} EPR signal of a 155:1 digal:Cr^{VI} mixture grows and decays at 20 °C (Fig. 11).

The rate constants for the formation and disappearance of the intermediate Cr^{V} were calculated from the variation of the intensity of the EPR signal versus time, and the k_6 and k_5 values were obtained using Eq. (3) derived from Scheme 1 for the total Cr^{V} in the mixture at any time.

$$h = A\,k_6(\exp(-2k_6t) - \exp(-k_5t))/(k_5 - 2k_6) \quad (3)$$

where A depends on the spectrometer settings (gain, power, modulation, etc.).

In the range of substrate employed in this work, plots of k_6 and k_5 versus [trigal] and [digal] gave good straight lines from which values of k_{6h} and k_{5h} were determined (Fig. 12).

For 0.2 M $HClO_4$ the rate laws for the Cr^{VI} and Cr^{V} disappearance are then given by

$$-d[Cr^{VI}]/dt = 2k_{6h}[S][Cr^{VI}] \text{ and } -d[Cr^{V}]/dt = k_{5h}[S][Cr^{VI}]$$

where $k_{6h} = 0.027(3)\ M^{-2}\ s^{-1}$; $k_{5h} = 0.013(1)\ M^{-2}\ s^{-1}$ and S = digal

where $k_{6h} = 0.024(2)\ M^{-2}\ s^{-1}$; $k_{5h} = 0.010(1)\ M^{-2}\ s^{-1}$ and S = trigal

The fact that CrO_2^{2+} was detected in the redox reaction of digal and trigal with Cr^{VI}, coupled with the observation of Cr^{V} species and the successful trapping of organic radicals using acrylonitrile

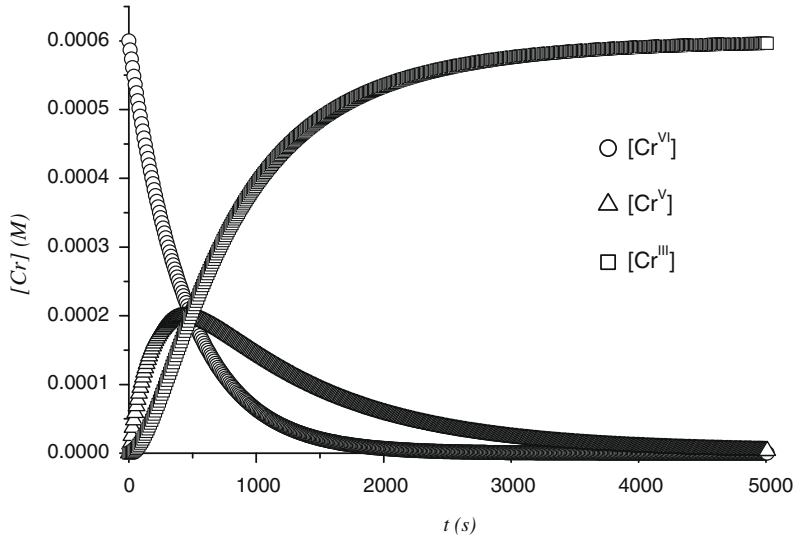

Fig. 10. Simulated kinetics profiles for Cr species. [Cr] calculated using k_6 = 0.00224 s^{-1}, k_5 = 0.00093 s^{-1}; [trigal] = 0.09 M; [$HClO_4$] = 0.20 M; T = 33 °C; I = 1.0 M; $[Cr]_T$ = 0.6 mM.

Table 4
Observed pseudo-first-order rate constants (k_6 and k_5) for different concentrations of digal–trigal at [$HClO_4$] 0.20 M.

[Digal or trigal] (M)	0.03	0.048	0.06	0.09
	$10^3\ k_6/s^{-1}$			
Digal	0.86(9)	1.3(1)	1.6(2)	2.4(2)
Trigal	0.69(7)	1.2(1)	1.4(1)	2.2(2)
	$10^3\ k_5/s^{-1}$			
Digal	0.36(4)	0.61(6)	0.81(8)	1.2(1)
Trigal	0.28(3)	0.52(5)	0.61(6)	0.93(9)

T = 33 °C; $[Cr^{VI}]_0$ = 0.6 mM; I = 1.0 M.

indicated that reaction occured through both one and two electron pathways involving Cr^{IV} and Cr^{V} intermediates species. However, under conditions employed in the kinetics measurements, Cr^{IV} reacted with digal and trigal faster than Cr^{VI} and does not accumulate in the reaction mixture. Therefore, Cr^{IV} should be involved in fast steps of the reaction pathway. In Scheme 2, a mechanism is proposed which combines $Cr^{VI} \rightarrow Cr^{IV} \rightarrow Cr^{II}$ and $Cr^{VI} \rightarrow Cr^{IV} \rightarrow Cr^{III}$ pathways, and takes into account: (a) kinetics results, (b) the polymerization test of acrylonitrile, (c) detection of oxo-Cr^{V} intermediates by EPR (d) observation of CrO_2^{2+}.

In the [$HClO_4$] under study, Cr^{VI} may exist as $HCrO_4^-$ [36], and this species is proposed as the reactive form of Cr^{VI}, in agreement with the first-order dependence of the reaction rate on [Cr^{VI}]. It is known that the chromic oxidation of alcohols, glycols and dicarboxylic acids are preceded by the formation of a chromate ester [36,37], so we proposed that the first step of the mechanism in Scheme 2 involves the formation of sustrate-Cr^{VI} mono-chelate (Eq. (4)), this chromate ester should be formed rapidly prior to the redox steps. The formation of the chromate ester is followed by the slow redox step where the C–C bond cleavage is proposed to occur through an acid catalyzed two-electron redox process to yield Cr^{IV}, HCO_2H and oxidized substrate (Eq. (5)).

The formation of Cr^{IV} was consistent with the observation of CrO_2^{2+}, the product of the reaction of Cr^{II} with O_2, which is taken as evidence of the Cr^{IV} formation [27,28]. After the slow redox step,

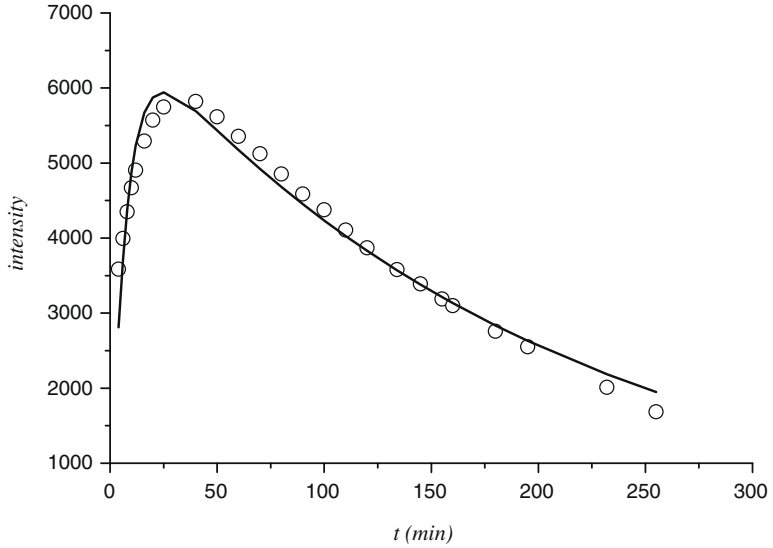

Fig. 11. Intensity of Cr^{V} EPR signals vs. time. [Cr^{VI}] = 0.97 mM, [digal] = 0.15 M [$HClO_4$] = 0.1 M, I = 1.0 M; T = 20 °C; mod. amp. = 2.0 G.

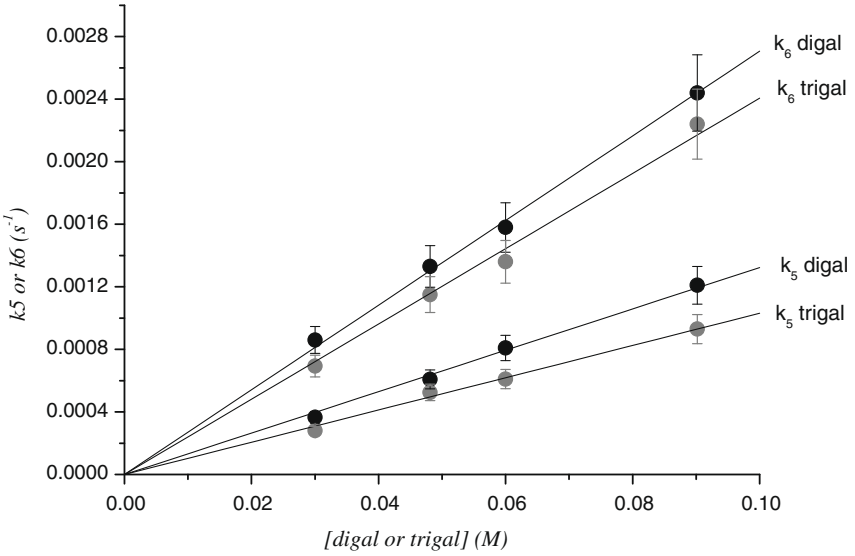

Fig. 12. Effect of [digal or trigal] on k_6 and k_5 at 33 °C; I = 1.0 M at [$HClO_4$] 0.2 M.

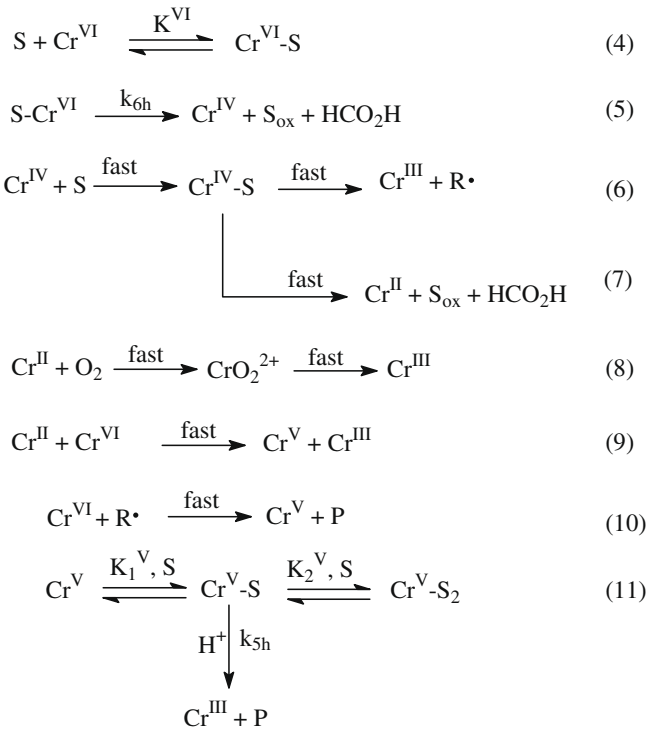

Scheme 2.

Cr^{IV} is predicted to react with excess substrate to yield Cr^{III} and radical or Cr^{II} and oxidize substrate through two alternative fast steps (Eqs. (6) and (7)). The first parallel step was supported by the observed polymerization of acrylonitrile when it was added to the reaction mixture, while the second one, by the formation of CrO_2^{2+}. Cr^{V} was produced by fast reaction of Cr^{II} with Cr^{VI} Eq. (9). Under the conditions used in the kinetic experiments, Eq. (8) can be neglected. The kinetic data indicate that Cr^{V} formed in the fast steps can further oxidize digal and trigal through an acid catalyzed step to yield Cr^{III} and the oxidized substrate as the final redox products. In Scheme 2, it is proposed that Cr^{V} reacts with digal or trigal to form an oxo-Cr^{V}-digal/trigal monochelate that yields the redox products through an acid catalyzed step ((11)). This proposal is in agreement with the EPR spectra at $[HClO_4]$ 0.20 M.

3.4. Cr^{VI} reduction and Cr^{III} retention by polygal

The redox reaction between Cr^{VI} and polygal and the tendency of the polysaccharide matrix in retaining Cr^{III} coming from redox reaction was studied. Under strong acidic media, polygal was fully protonated producing insoluble aggregates which consist in polymer chains joined by hydrogen bonds between the carboxyl and hydroxyl groups [38]. At pH 7.00, the polymer was soluble, due to the presence of deprotonated carboxylate groups. Speed of aggregation depends on the experimental conditions (acidity, temperature, shaking, etc.) and was standardized in order to obtain particles of uniform size. Reaction mixture of polygal/Cr^{VI} was performed keeping $[Cr^{VI}]$, $[HClO_4]$ and temperature constant. The amount of polygal was varied between 25 and 1200 mg. Absorbance measurements at 350 nm versus time performed on mixtures polygal/Cr^{VI} showed the disappearance of Cr^{VI}. At the same time, absorbance values at 570 nm did not show the corresponding increment of Cr^{III} because it was capturated on the solid matrix of the polymer as a cyan-coloured solid. The polygal efficiency in Cr^{III} retention – coming from the reduction of Cr^{VI} – was defined in Eq. (12) as *%E*.

$$\%E = 100 \times \left([Cr^{VI}]_0 - [Cr]_{final}\right)/[Cr^{VI}]_0 \quad (12)$$

Fig. 13 and Table 5 show the obtained results varying the mass of polygal.

As we can see, employing 990 mg of polygal, *%E* is almost 90%. Increasing the amount of polygal from 990 to 1200 mg does not produce a significative increment on the *%E* value. The chromium analysis on the solid, confirm the results of the supernatant. For the experience with 1200 mg of polygal, analysis of the solid afforded 23 mg Cr per solid g, which represents 88.5% of the initial $[Cr^{VI}]_0$ coincident with the value showed in Table 5, considering the experimental error. The efficiency of polygal for eliminating Cr was higher, as demonstrated in the determination of *%E* at different times even though the speed of redox process was low. Considering an amount of 780 mg polygal, in the experimental conditions of Table 5, the *%E* was 39.0 and 74.0 for 3.0 and 10 h, respectively. In order to check if the speed of reduction of $[Cr^{VI}]$ by polygal was the limiting process of the reaction, the same

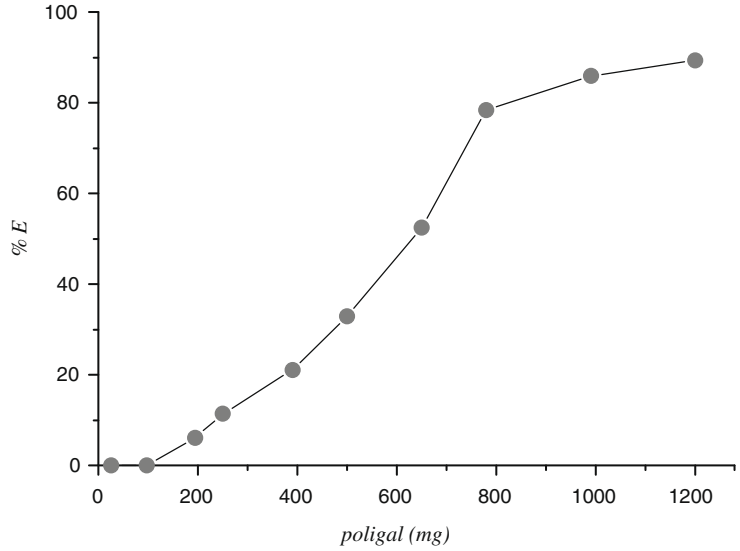

Fig. 13. Effect of [polygal] on *%E* at 60 °C; *I* = 1,0 M, *t* = 24 h at $[HClO_4]$ 0.12 M.

Table 5
Effect of [polygal] on %*E* at 60 °C; *I* = 1.0 M, *t* = 24 h at [$HClO_4$] 0.12 M.

Polygal (mg)	$[Cr]_f$ (mM)	%*E*
1200	1.86	89.4
990	2.46	87.0
780	3.80	78.4
650	7.64	56.6
500	11.79	33.0
390	13.45	23.6
250	15.35	12.8
195	16.30	7.4
97.5	17.6	0
25	17.6	0

reaction mixture added with 0.9 mmol Na_2SO_3 was prepared. The reduction of Cr^{VI} to Cr^{III} was almost instantaneous and the %*E* value reached 90%, practically the same value obtained after 24 h without the addition of Na_2SO_3. This result confirms that Cr^{VI} reduction was the limiting step in the chromium elimination by polygal.

3.5. Polygal/Cr^{VI} reactions mixture: oxidation product

The oxidation of polygal with Cr^{VI} afforded two products: HCO_2H (determined by HPLC) and CO_2 determined by titration in alkaline medium. The quantification of these products afforded 0.3 mol HCO_2H and 1.1 mol CO_2 per mol Cr^{VI}. According to the experimental conditions employed, the formic acid could react with Cr^{VI} affording CO_2. The last reaction is slower than Cr^{VI}-polygal reaction [39] and the concentration of HCO_2H was lower than the carboxylate groups in polygal. Consequently, the transformation of formic acid in CO_2 by oxidation with Cr^{VI} was discarded. In the proposed mechanism (Scheme 3), if the consecutive steps (ii) and (iii) occur in the same proportion then, the stoichiometry of the global reaction could be written as the following reaction (Eq. (13)).

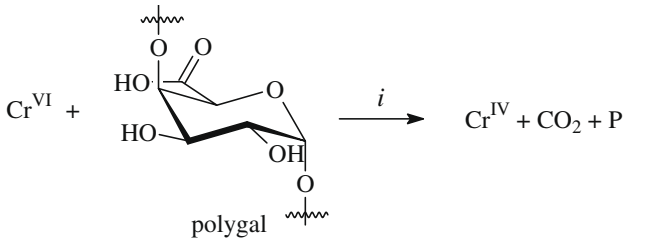

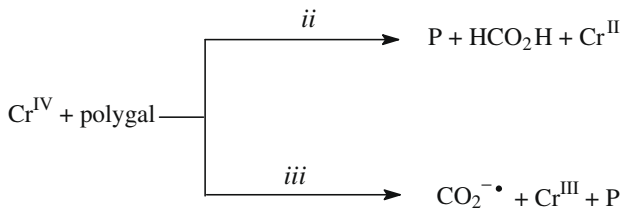

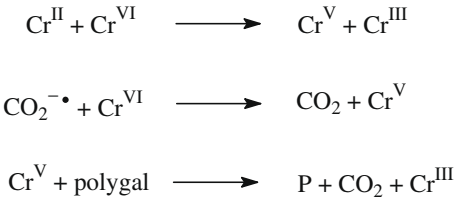

Scheme 3.

$$Cr^{VI} + 1.5\ \text{polygal} \rightarrow Cr^{III} + 1.5\ P + 1.25\ CO_2 + 0.25\ HCOOH \quad (13)$$

According to this stoichiometry, 1.25 mol of CO_2 and 0.25 mol of HCOOH per mol of Cr^{VI} should be produced, which is in agreement with the experimental results. The absence of signals belonging to monomers or oligomers of low molecular weight in the HPLC chromatograms of the supernatant reaction mixture, discarded the participation of the glucosidic linkage α (1–4) in the redox reaction with Cr.

Scheme 3 adjusts the reaction mechanism for oxidation of oxygenated compounds with Cr^{VI}, in agreement with sequences combination: $Cr^{VI} \rightarrow Cr^{IV} \rightarrow Cr^{II}$ and $Cr^{VI} \rightarrow Cr^{IV} \rightarrow Cr^{III}$.

4. Conclusions

The results presented in this report showed that digal, trigal and polygal were able to reduce Cr^{VI} to Cr^{III}. The redox reaction took place through the combination of $Cr^{VI} \rightarrow Cr^{IV} \rightarrow Cr^{II}$ and $Cr^{VI} \rightarrow Cr^{IV} \rightarrow Cr^{III}$ pathways related with Cr^{V} and radical species in digal–trigal/Cr^{VI} mixtures.

Besides, in this report the results evidence that polygal was able to reduce Cr^{VI} to Cr^{III} and trap efficiently the last form of chromium, so it turns out to be an interesting model for the study of biomaterials which possess a high proportion of this polymer in its composition. Since polygal is better as a Cr^{III} chelating agent than as a reducing agent of Cr^{VI}; the elimination of chromium from contaminated waste water could be more efficient employing biomaterial containing polygal. The results obtained are particularly important because the majority of the chromium remediation methods employed so far are meant for the reduction Cr^{VI} to Cr^{III}; without considering the free Cr^{III} in solution. Due to the fact that Cr^{III} could be oxidized biologically [40] or chemically under extreme environmental conditions [41], new methods of elimination of chromate from water should consider the elimination of chromium in both oxidation states [9].

EPR measurements show that species where Cr^{V} bounds to a ligand through the α-alcoxocarboxylate groups (or 2-O^{ring} carboxylate) predominate in acidic medium, meanwhile at pH 7.0 the species $[Cr^{V}O(\textit{cis}\text{-diolate})_2]^-$ predominate, as can be seen on aldonic acids, others uronic acids and polyhidroxocarboylic compounds [18,20,25].

Acknowledgements

We thank the National Research Council of Argentina (CONICET); the National University of Rosario (UNR); the ALFA Program (CROCON Network ProjetALR/B7-30.11/94-7.0064.9); Secyt (Argentina) – OMFB (Hungary) bilateral agreement (project HU / A98-EVI/07); Secyt (Argentina)-Conicyt (Chile) bilateral Agreement (projet HC-PA/01-E04).

References

[1] B. Ridley, M. ÓNeill, D. Mohnen, Phytochemistry 57 (2001) 929.
[2] S. Angyal, Chem. Soc. Rev. 10 (1980) 415.
[3] S. Deiana, L. Erre, G. Micera, P. Piu, Inorg. Chim. Acta 46 (1980) 249.
[4] G. Micera, S. Deiana, Inorg. Chim. Acta 56 (1981) 109.
[5] A. Nguyen, I. Mulyani, A. Levina, P. Lay, Inorg. Chem. 46 (2008) 4299.
[6] S. Rengaraj, K. Yeon, S. Moon, J. Hazard. Mater. B87 (2001) 273.
[7] V. Konovalova, G. Dmytrenko, R. Nigmatullin, M. Bryk, P. Gvozdyak, Enzime Microb. Technol. 33 (2003) 899.
[8] S. Bailey, T. Olin, R. Bricka, D. Adrian, Water Res. 33 (1999) 2469.
[9] S. Bellú, S. García, Juan C. González, Ana M. Atria, Luis F. Sala, S. Signorella, Separation Sci. Technol. 43 (2008) 3200.
[10] International Agency for Research on Cancer (IARC), IARC Monogr. Eval. Carcinog. Risk Chem. Hum. 2 (Suppl. 7) (1987) 165.
[11] R. Feldam, Occupational and Environmental Neurotoxicology, Lippincott-Raven Publishers, Philadelphia, PA, 1999. p. 337.

[12] S.B. Asif, D. Dollimore, Thermochím. Acta 77 (1984) 395.
[13] WinSIM EPR calculations for MS-Windows, version 0.96: National Institute of Environmental Health Sciences, 1995.
[14] M. Krumpolc, J. Rocek, Inorg. Synth. 20 (1980) 63.
[15] M.C. Ghosh, E.S. Gould, Inorg. Chem. 30 (1991) 491.
[16] F. Feil, Spot Test in inorganic analysis, Elsevier, London, 1982. p. 341.
[17] A.B.P. Lever, in: Inorganic Electronic Spectroscopy, second ed., Elsevier, Amsterdam, 1984, p. 419.
[18] R. Codd, C.T. Dillon, A. Levina, P.A. Lay, Coord. Chem. Rev. 216/217 (2001) 537.
[19] M. Rizzotto, A. Levina, M. Santoro, S. García, M. Frascaroli, S. Signorella, L. Sala, P.A. Lay, J. Chem. Soc., Dalton Trans. (2002) 3206.
[20] S. Signorella, J. González, L. Sala, J. Argentine Chem. Soc. 90 (2002) 1.
[21] G. Barr-David, M. Charara, R. Codd, R. Farrell, J. Irwin, P. Lay, R. Bramley, S. Brumby, J.-Y. Ji, G. Hanson, J. Chem. Soc., Faraday Trans. 91 (1995) 1207.
[22] R. Bramley, J.-Y. Ji, R.J. Judd, P.A. Lay, Inorg. Chem. 29 (1990) 3089.
[23] R.P. Farrell, R.J. Judd, P.A. Lay, R. Bramley, J.-Y. Ji, Inorg. Chem. 28 (1989) 3401.
[24] C. Gouvión, K. Mazeau, A. Heyraud, F. Taravel, I. Tvaroska, Carbohydr. Res. 261 (1994) 187.
[25] J.C. González, V. Daier, S. García, B.A. Goodman, L.F. Sala, S. Signorella, Dalton Trans. 15 (2004) 2288.
[26] S. Scott, A. Bakac, J. Espenson, J. Am. Chem. Soc. 113 (1991) 7787.
[27] S. Scott, A. Bakac, J. Espenson, J. Am. Chem. Soc. 114 (1992) 4205.
[28] A. Al-Ajlouni, A. Bakac, J.H. Espenson, Inorg. Chem. 33 (1994) 1011.
[29] J. Pérez Benito, C. Arias, D. Lamrhari, New J. Chem. 18 (1994) 663.
[30] J. Pérez Benito, C. Arias, Can. J. Chem. 71 (1993) 649.
[31] J. González, S. García, N. Mamana, L.F. Sala, S. Signorella, Inorg. Chem. Commun. 9 (2006) 437.
[32] F. Mangiameli, J.C. González, S. García, S. Bellú, S. Signorella, L.F. Sala, unpublished results.
[33] S. Bellú, J. González, S. García, S. Signorella, L.F. Sala, J. Phys. Org. Chem. 21 (2008) 1059.
[34] G.P. Haight, G.M. Jursich, M.T. Kelso, P.J. Merrill, Inorg. Chem. 24 (1985) 2740.
[35] R.G. Wilkins, The Study of Kinetics and Mechanism of Reactions of Transition Metal Complexes, Allyn & Bacon, Boston, 1974. p. 20.
[36] M. Mitewa, P. Bontchev, Coord. Chem. Rev. 61 (1985) 241.
[37] J.K. Beattie, G.P. Haight, in: J.O. Edwards (Ed.), Inorganic Reaction Mechanisms. Part II, Wiley, New York, 1972.
[38] M. Alonso-Mougán, F. Fraga, F. Meijide, E. Rodriguez-Nuñez, J. Vázques-Tato, Carbohydrate Polymers 51 (2003) 37.
[39] C. Arias, J.F. Pérez-Benito, Collect. Czech. Chem. Commun. 57 (1992) 1821.
[40] A. Nguyen, I. Mulyani, A. Levina, P.A. Lay, Inorg. Chem. 47 (2008) 4299.
[41] A.D. Apte, S. Verma, V. Tare, P. bose, Journal of Hazardous Materials B121 (2005) 215.